Electronic Supplementary Material (ESI) for Nanoscale.
This journal is © The Royal Society of Chemistry 2017

Supplementary Information

Spatially Controlled Positioning of Coordination Polymer Nanoparticles onto Heterogeneous Nanostructured Surfaces.

V. Trannoy,[1] M. Faustini,[2] D. Grosso,[2,†] F. Brisset,[1] P. Beaunier,[3] E. Rivière,[1] M. Putero,[4] A. Bleuzen[1]

[1]Institut de Chimie Moléculaire et des Matériaux d'Orsay, CNRS, Université Paris-Sud, Université Paris-Saclay, 91400 Orsay, France.

[2] Sorbonne Universités, UPMC Univ Paris 06, CNRS, Collège de France, UMR 7574, Chimie de la Matière Condensée de Paris, F-75005, Paris, France

[3] Sorbonne Universités, UPMC Univ Paris 06, CNRS, UMR 7197, Laboratoire de Réactivité de Surface, F-75005, Paris, France

[4] Institut Matériaux Microélectronique et Nanosciences de Provence, (IM2NP) - UMR CNRS 7334, Aix-Marseille Université, Faculté des Sciences de Saint Jérôme, 13397 Marseille Cedex 20, France.

Figure S1: AFM image of the nanoperforated titania film deposited onto the gold layer.

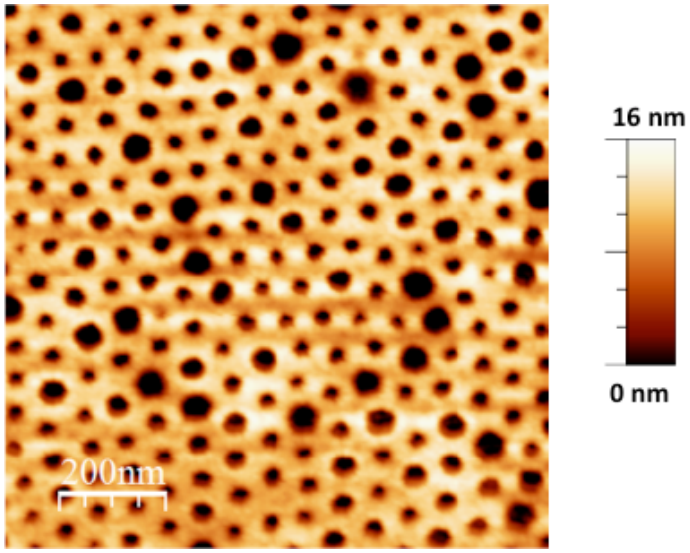

Figure S2: Grazing-Incidence Small-Angle X-ray Scattering of a) the TiO_2 nanoperforated film, b) the TiO_2 nanoperforated film after PBA particles formation and corresponding AFM images of c) the TiO_2 nanoperforated film and d) the TiO_2 nanoperforated film after PBA particles formation.

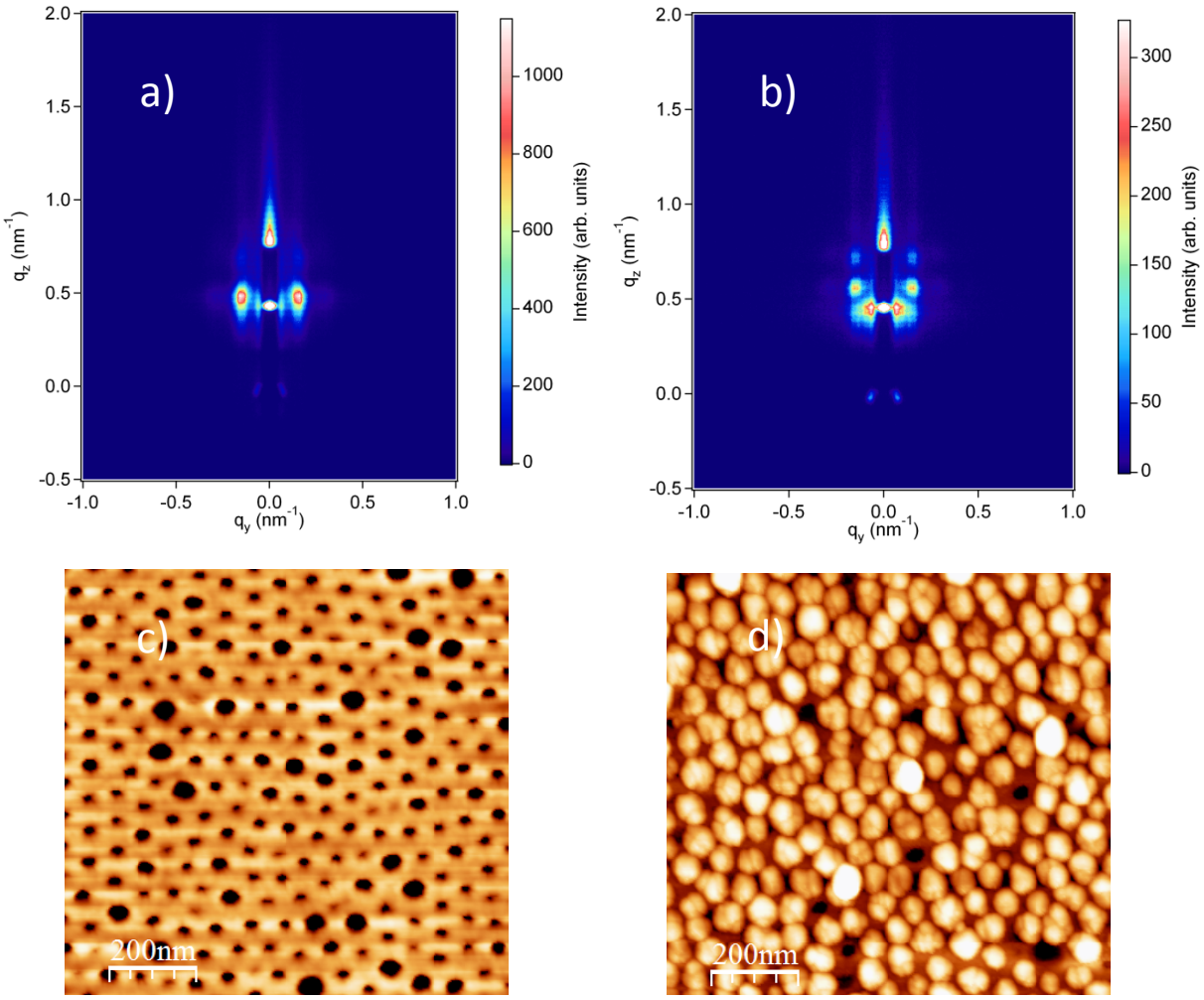

Figure S3: FT-IR spectrum of the film before and after the cycles of immersions in PBA precursors solutions.

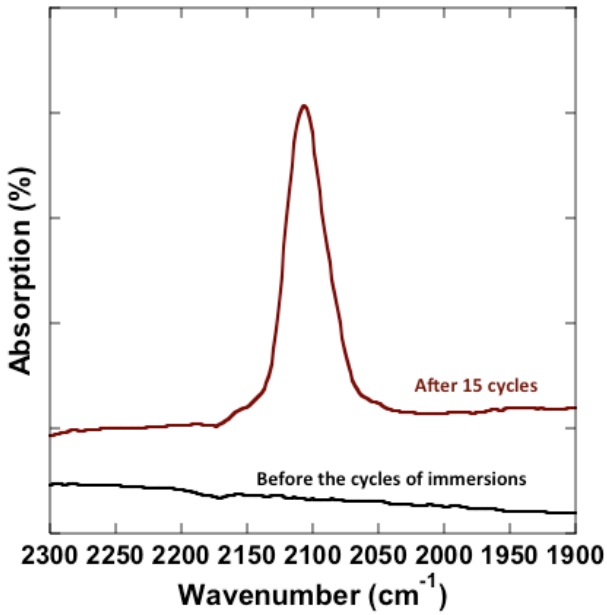

The appearance of the band at 2106 cm^{-1} assigned to cyanide in Co-NC-Fe linkages confirms the formation of PBA particles. The narrow line-width is in line with well-crystallized PBA particles. Fourier Transform-Infrared (FT-IR) spectra were collected in the attenuated total reflection (ATR) mode using a Vertex 70 spectrometer with a germanium crystal.

Figure S4: SEM image of **Au-PTiO$_2$-15C**.

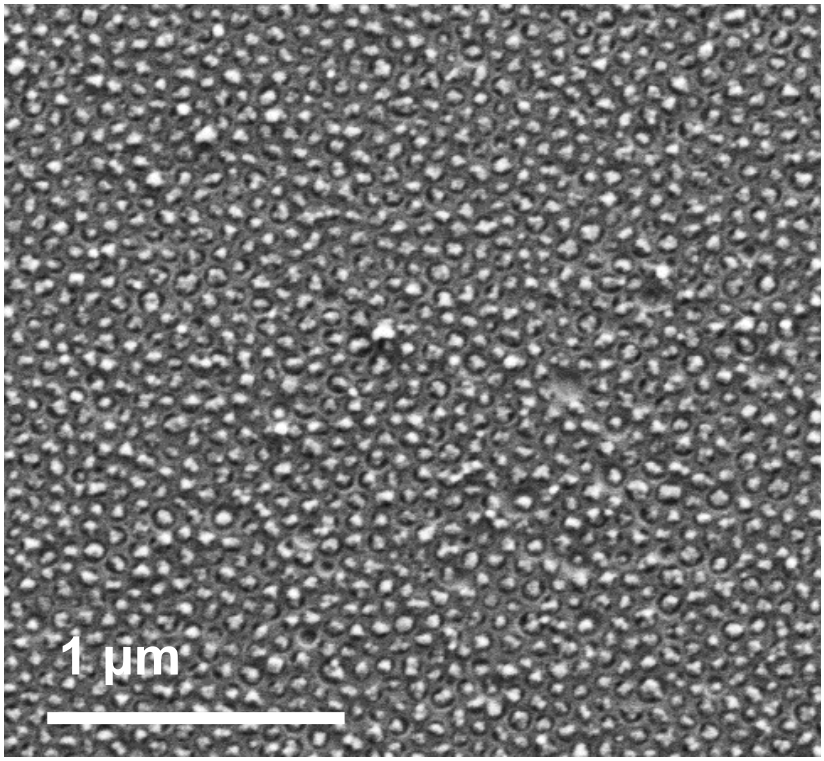

The nanoperforations are filled with PBA particles over a large surface area.

Figure S5: SEM images of **Au-PTiO$_2$-15C** (right image) and of the film obtained by the previously described layer-by-layer growth method (left image). Following the previous approach, all the perforations are not filled with PBA particles (black arrows indicate empty nanoperforations) and the islands of PBA filling the perforations are not all isolated from each other (the black circle surrounds aggregated PBA islands).

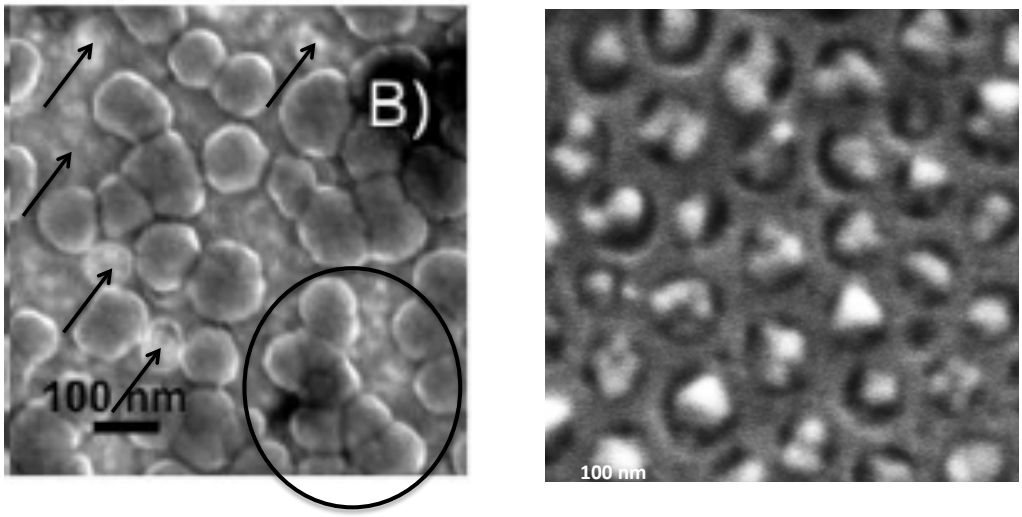

Figure S6: AFM images of a) **Au-PTiO$_2$-1C** and b) **Au-PTiO$_2$-2C** and example of height profile along a line passing through one perforation of c) **Au-PTiO$_2$-1C** and of d) **Au-PTiO$_2$-2C**.

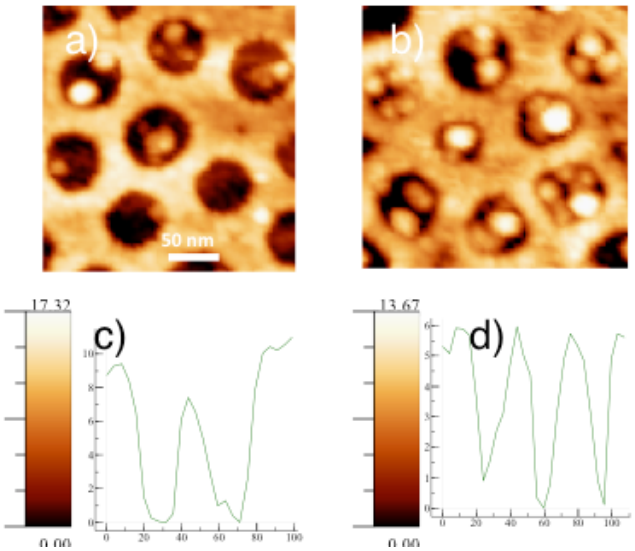

Figure S7: AFM image of **PTiO$_2$-1C** (a) compared to the AFM image of **Au-PTiO$_2$-1C** (b).

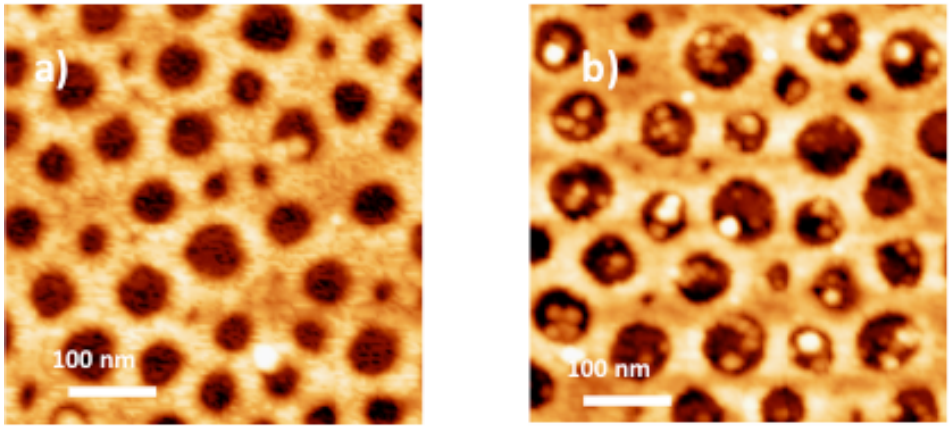

In order to unravel the impact of the gold layer on the nucleation process, the first cycle of immersions was performed on the titania nanoperforated layer directly deposited onto the native SiO_2 of the silicon substrate called **PTiO$_2$-1C**. Much fewer particles are formed when the native SiO_2 layer on the silicon wafer replaces the gold layer. Therefore, one can conclude that the presence of the gold layer strongly favours the nucleation process by lowering the nucleation activation energy. The localization of the particles within the nanoperforations and their formation in larger amounts on that surface can be assigned to a heterogeneous nucleation process favoured on the gold surface.

Since only very few PBA particles were formed on the continuous Au film (**Au-15C**, Figure 2a) whereas this surface favours PBA nucleation, one can conclude that most of the PBA molecular precursor species are washed away from this surface during the rinsing step. In contrast, the amount of PBA particles formed on the continuous TiO_2 film (**CTiO$_2$-15C**, Figure 2b) is slightly but significantly larger than on the continuous Au film (**Au-15C**, Figure 2a). As the nucleation activation energy is higher on this surface, this suggests a higher retention rate of PBA molecular precursor species, most probably Co^{2+} species, than on the Au film.

Figure S8: Experimental and fitted GIXRD on **Au-PTiO$_2$-15C** after thermal annealing at an incident angle ω = 1°. The fit was performed using Lorenztian functions.

Fig.S8 shows the experimental GIXRD recorded at an incident angle ω = 1°. The experimental curve can only be fitted with a combination of 2 peaks indicating the presence of both Au and CoFe crystalline domains in this diffraction line. The diffraction peak corresponding to (110) CoFe planes was found at 2θ = 44.74° leading to a lattice plane spacing (0.202±0.001 nm), consistent with (110) d-spacing of the CoFe metal alloy cubic phase (Powder Diffraction File # 49-1568).

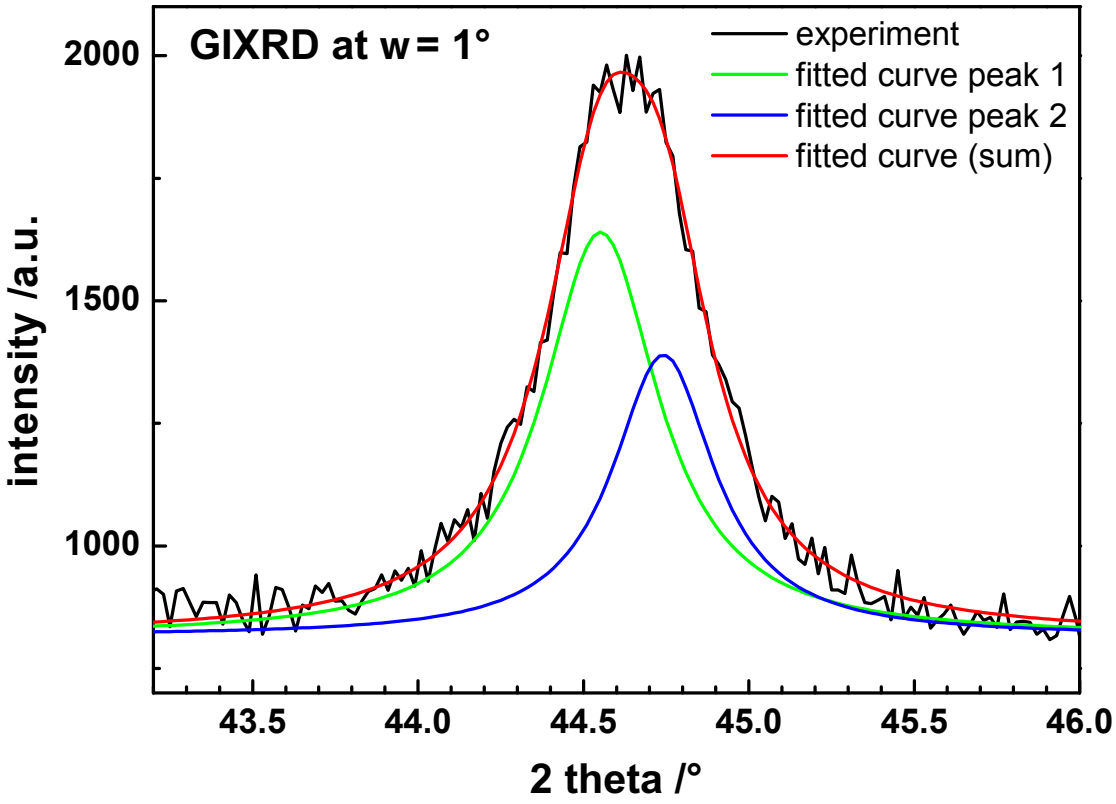

Figure S9: Field-cooled and zero-field-cooled magnetization curves of **Au-PTiO$_2$-15C**.

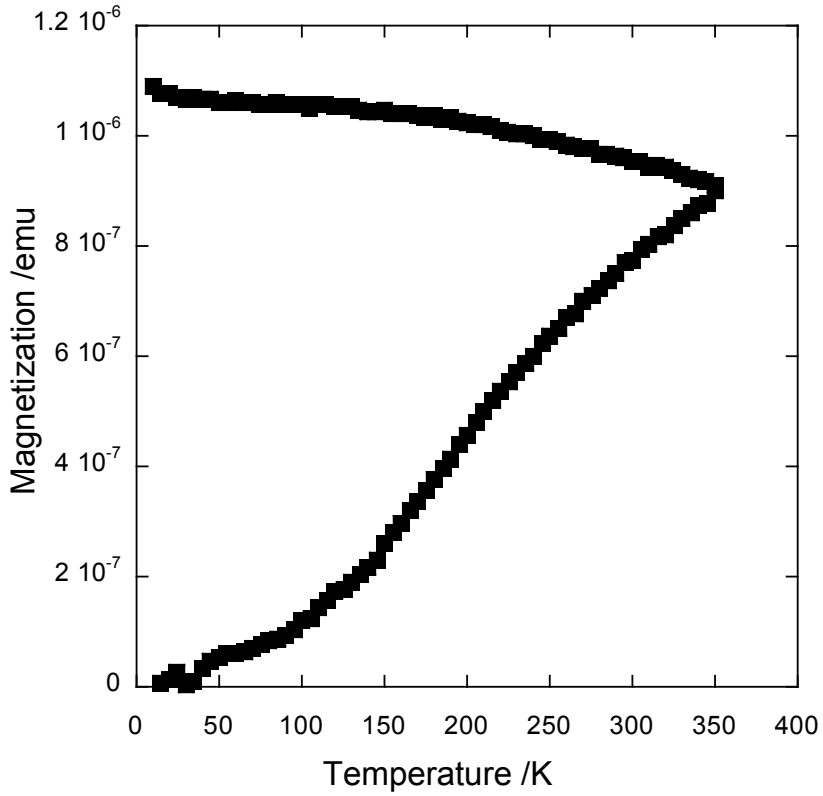

Figure S10: Magnetic field dependence of the magnetization of **Au-PTiO$_2$-15C** at 10 K and at 300 K. The film exhibits ferromagnetic, super ferromagnetic or super spin-glass behavior at 10K and 300K.